NMR and EPR Investigations of Iron Corrolates: Iron(III) Corrolate π Cation Radicals or Iron(IV) Corrolates?

Sheng Cai,[†] F. Ann Walker,*[,†] and Silvia Licoccia*[,‡]

Department of Chemistry, University of Arizona, Tucson, Arizona 85721-0041, and Dipartimento di Scienze e Tecnologie Chimiche, Universitá di Roma Tor Vergata, Via della Ricerca Scientifica, 00133 Rome, Italy

Received July 1, 1999

The chloroiron corrolates of 2,3,7,8,12,13,17,18-octamethyl- and 7,13-dimethyl-2,3,8,12,17,18-hexaethylcorrole ([(Me_8C)FeCl] and [(7,13-Me_2Et_6C)FeCl], respectively) and their bisimidazole complexes have been investigated by NMR spectroscopy as a function of temperature, and by EPR spectroscopy at 4.2 K. Magnetic susceptibilities were measured by the modified Evans method. It is found that the electron configuration of the chloroiron corrolates is that of a $S = 3/2$ Fe(III) center coupled to a corrolate π radical, where one electron has been removed from the π system of the corrolate. This π radical is antiferromagnetically coupled to the unpaired electrons of the iron to yield an overall $S = 1$ complex, as evidenced by the very large positive shifts of the *meso*-H resonances (183 and 172 ppm). That this antiferromagnetic coupling is very strong is supported by the near-Curie behavior of the ^{1}H chemical shifts. For the chloroiron corrolates in the presence of imidazole, imidazole-d_4, and *N*-methylimidazole at temperatures of −50 °C and below, the mono- and bisligand complexes are formed. The NMR spectra can be assigned on the basis of chemical exchange between the chloroiron(III) parent complex and the bisligand complex at −30 °C, and between the bisligand complex and the monoligand complex at −50 °C. The bisimidazole complexes show pyrrole CH_2 and CH_3 resonances characteristic of low-spin Fe(III) centers ($S = 1/2$), but with strongly upfield-shifted *meso*-H resonances (δ values of −95 and −82.5 ppm for the octamethyl complex and −188 and −161 ppm for the dimethylhexaethyl complex at 203 K) characteristic of the presence of a macrocycle-centered unpaired electron. The magnetic moments of these bisligand complexes are somewhat lower than expected for overall $S = 1$ systems, and decrease as the temperature is lowered. The lower apparent magnetic moments (2.0−1.8 μ_B between −50 and −90 °C) are believed to be caused by a combination of weak or no magnetic coupling between the metal and macrocycle electrons and decreasing solubility of the complex as the temperature is lowered. The non-Curie behavior of the ^{1}H chemical shifts observed in the low-temperature (−50 to −90 °C) NMR spectra likely arises from a combination of the effects of weak antiferromagnetic coupling of metal and macrocycle spins, a low-lying electronic excited state, and ligand binding/loss equilibria at the highest temperatures studied (−50 °C).

Introduction

Considerable interest has arisen recently concerning non-porphyrin tetrapyrrole macrocycles. Such systems are completely synthetic but bear structural resemblance to the naturally occurring porphyrins, so that they have been classified as contracted, isomeric, or expanded porphyrins. However, their physical and chemical characteristics are quite different because of the modifications introduced in the peripheral skeleton of the macrocycle.[1,2] Among such modified porphyrins, the one for which the richest coordination chemistry has been developed is corrole.[3−7] Numerous metal ions have been coordinated to corroles to form complexes which are essentially planar even in the presence of β- and *meso*-substituents. Corroles lack a *meso*-carbon bridge but retain an 18-electron aromatic π-system, and have been considered to have structures intermediate between those of corrins, the nucleus of coenzyme B_{12}, and porphyrins, the prosthetic groups of heme proteins. At variance with a porphyrin, corrole is a trianionic ligand and its cavity is slightly smaller. It has thus been considered ideal for chelating small, high-valent first-row transition metals.[2,8] Studies on the electronic structures of several metallocorrolates have shown, however, that it is very easy to remove one π-electron from the

[†] University of Arizona.
[‡] Universitá di Roma Tor Vergata.

(1) Sessler, J. L.; Weghorn, S. J. *Expanded, Contracted and Isomeric Porphyrins*; Tetrahedron Organic Chemistry Series Vol. 15; Pergamon: Oxford, 1997; pp 1−503.
(2) Vogel, E. *J. Heterocycl. Chem.* **1996**, *33*, 1461.
(3) Licoccia, S.; Paolesse, R. In *Metal Complexes with Tetrapyrrole Ligands III*; Buchler, J. W., Ed.; Springer-Verlag: Berlin, Germany, 1995; Vol. 84, pp 73−133.
(4) Licoccia, S.; Paolesse, R.; Tassoni, E.; Polizio, F.; Boschi, T. *J. Chem. Soc., Dalton Trans.* **1995**, 3617.
(5) Murakami, Y.; Yamada, S.; Matsuda, Y.; Goto, T.; Kuramoto, M. *Rep. Asahi Glass Found. Ind. Technol.* **1979**, *34*, 295.
(6) Tse, M. K.; Zhang, Z.; Mak, T. C. W.; Chan, K. S. *J. Chem. Soc., Chem. Commun*. **1998**, 1199.
(7) Paolesse, R.; Boschi, T.; Licoccia, S.; Khoury, R. G.; Smith, K. M. *J. C. S. Chem. Commun.* **1998**, 1119.
(8) Vogel, E.; Will, S.; Schulze Tilling, A.; Neumann, L.; Lex, J.; Bill, E.; Trautwein, A. X.; Wieghardt, K. *Angew. Chem., Int. Ed. Engl.* **1994**, *33*, 731.
(9) Will, S.; Lex, J.; Vogel, E.; Schmickler, H.; Gisselbrecht, J. P.; Haubtmann, C.; Bernard, M.; Gross, M. *Angew. Chem., Int. Ed. Engl.* **1997**, *36*, 357.
(10) Licoccia, S.; Morgante, E.; Paolesse, R.; Polizio, F.; Senge, M. O.; Tondello, E.; Boschi, T. *Inorg. Chem.* **1997**, *36*, 1564.
(11) Will, S.; Lex, J.; Vogel, E.; Adamian, V. A.; Van Caemelbecke, E.; Kadish, K. M. *Inorg. Chem.* **1996**, *35*, 5577.

10.1021/ic990784l CCC: $19.00
Published on Web 07/12/2000

macrocycles, and that these species can be formulated as complexes of a formally reduced metal ion bound to a corrole cation radical.[9−11] In some cases, modifications of the electronic ground state may be induced by axial ligation.

The electronic configuration of the central metal atom controls the physical and chemical properties of tetrapyrrole metal complexes.[12−17] For paramagnetic systems, EPR and NMR spectroscopies provide complementary information about orbital occupation and relative energies, and have been widely used to investigate in great detail synthetic iron porphyrinates.[14−18] The magnetic properties of these complexes can be altered significantly by the nature of the axial ligands. For a series of pyridine complexes of tetramesitylporphyrinatoiron(III) it has been found that, as the basicity of the pyridine ligands decreases, the electronic ground state (always low-spin, $S = 1/2$) shifts from the $(d_{xy})^2(d_{xz},d_{yz})^3$ configuration commonly observed for heme proteins to the novel $(d_{xz},d_{yz})^4(d_{xy})^1$ configuration now recognized as important for the iron complexes of some of the "reduced hemes", the iron isobacteriochlorins and β-dioxoporphyrins (also known as dioxoisobacteriochlorins), such as heme d_1.[14−21] With less sterically demanding porphyrins, conversion to higher spin state complexes has been reported for the pyridine complex itself at room temperature and above.[22] Spectroscopic studies on iron(III) corrolates in pyridine solution indicate that a similar tendency toward higher spin states is also evident for this macrocycle,[3,23] but no data have been published on the binding of nitrogenous bases other than pyridine, or for the 1-electron oxidized chloroiron corrolates. We have therefore undertaken a NMR and EPR spectroscopic study of iron corrolates to compare their properties with those of iron porphyrinates and determine the electronic ground state stabilized by ligation of iron to a corrole.[24] Considerable information has already been reported concerning the supposed electronic ground state determined by Mössbauer spectroscopy,[8,23] but as we will show, zero-field Mössbauer spectra at 77 K may not be unique for differentiating an iron(IV) corrolate from an iron(III) corrole cation radical, whereas NMR spectroscopy is able to make a definite assignment. As a part of our study, we have investigated the NMR and EPR spectra of the bisimidazole complex of several iron corrolates, and find that the spin state and mode of electron coupling are different in these cases.

Experimental Section

Materials and Sample Preparation. 2,3,7,8,12,13,17,18-Octamethylcorrole [$(Me_8C)H_3$] and 7,13-dimethyl-2,3,8,12,17,18-hexamethylcorrole [$(7,13\text{-}Me_2Et_6C)H_3$] were prepared as described previously.[3,4] The chloroiron derivatives $(Me_8C)FeCl$ and $(Me_2Et_6C)FeCl$ were prepared according to the procedure previously reported for the octaethyl derivative.[8] Imidazole and *N*-methylimidazole were purchased from Aldrich, and used as received. Deuterated imidazole, imidazole-d_4 (D, 98%), was purchased from Cambridge Isotope Laboratories. Complexes with imidazole ligands were prepared in 5 mm NMR tubes in deuterated methylene chloride, CD_2Cl_2 (Cambridge Isotope Laboratories), by directly adding excess CD_2Cl_2 solution of axial ligands (iron corrolate:axial ligand = 1:6 in moles). All samples were prepared immediately prior to the recording of NMR data without degassing.

NMR Spectroscopy. ^{1}H NMR spectra were recorded on a Varian Unity-300 spectrometer operating at 299.955 MHz with a variable-temperature unit. The spectra were taken in CD_2Cl_2 over temperature ranges from −85 to +30 °C, referenced by the resonance from residual solvent protons (5.32 ppm relative to TMS). The temperature was calibrated using the standard Wilmad methanol and ethylene glycol samples. 1D spectra were collected by using the standard one-pulse experiment with a spectral width of 60−70 kHz, a 90° pulse, and 256−1024 transients. In the case when the relative peak areas were needed to calculate the number of protons for each resonance, a long acquisition time of 1 s and long relaxation delay of 5 s were used. If no integral was needed, the acquisition time of 50−100 ms and zero relaxation delay were used.

DQF-COSY and NOESY spectra were acquired with a spectral window of 12−18 kHz using 512 t_2 data points, 128 t_1 increments, and 512−1024 transients with relaxation delays ranging from 0.1 to 0.3 s and mixing times of 20−40 ms. All data were processed on the workstation of the Unity-300, with a line-broadening window function (lb = 20) for 1D data and a Gaussian function for each dimension of the 2D data. For 2D spectra, zero-filling was used to give final matrixes of 1024 t_1 × 1024 t_2 data points before Fourier transformation.

EPR Experiments. The samples were the same as the ones prepared for NMR experiments. After NMR spectra were collected, the samples were transferred from NMR tubes directly to EPR tubes, and kept frozen in liquid nitrogen for EPR studies the following day. For quantitation of EPR signals, samples were prepared immediately before data acquisition. Samples of 0.010 mmol (5.8 mg for $[(7,13\text{-}Me_2Et_6C)FeCl]$, 7.6 mg for [(TMP)FeCl]) were weighed out and dissolved in 10 mL of CH_2Cl_2. For each sample, a small amount of solution was transferred to an EPR tube and a large excess of imidazole was added. The samples were frozen in liquid nitrogen. The EPR spectra were obtained on a CW EPR spectrometer ESP-300E (Bruker) operating at X-band using 0.2 mW microwave power and a 100 kHz modulation amplitude of 2 G. A Systron-Donner microwave counter was used for measuring the frequency. The EPR measurements were performed at 4.2 K using an Oxford continuous flow cryostat, ESR 900.

Magnetic Susceptibility Measurements. The magnetic susceptibility was measured by NMR methods on the Varian Unity-300 in the temperature range from −85 to +30 °C. This is a modification of the Evans method,[25] in which the equations have been modified for the geometry of a superconducting magnet.[26] A special coaxial tube (Wilmad) was used in this measurement. The solution of the paramagnetic complex was placed in the inner narrow-bore tube, and the solvent was placed in the outer tube, which is a regular NMR tube. The volume magnetic susceptibility (χ) of the paramagnetic compound was calculated from

$$\chi = \chi_0 + 750\Delta\nu/(\nu_0\rho c) \quad (1)$$

where χ_0 is the volume magnetic susceptibility of the pure solvent, $\Delta\nu$ (Hz) is the separation of the reference peaks (in this study, solvent was used as the reference) from the inner and outer tubes, ν_0 is the operating RF frequency of the spectrometer, ρ is the density of the

(12) La Mar, G. N.; Walker, F. A. In *The Porphyrins, Vol. IV*; Dolphin, D., Ed.; Academic Press: New York, **1979**; pp 61−157.
(13) Goff, H. In *Iron Porphyrins, Part I*; Lever, A. B. P., Gray, H. B., Eds.; Addison-Wesley: Reading, MA, 1983; pp 237−273.
(14) Walker, F. A.; Simonis, U. In *Biological Magnetic Resonance, Vol. 12: NMR of Paramagnetic Molecules*; Berliner, L. J., Reuben, J., Eds.; Plenum Press: New York, 1993; pp 133−274.
(15) Walker, F. A. *Coord. Chem. Rev.* **1999**, *185−186*, 471−534.
(16) Walker, F. A. Proton NMR and EPR Spectroscopy of Metalloporphyrins. In *The Porphyrin Handbook*; Kadish, K. M., Smith, K. M., Guilard, R., Eds.; Academic Press: Burlington, MA, 1999; Book 5, Chapter 36, pp 81−183.
(17) Nakamura, M.; Ikeue, T.; Fujii, H.; Yoshimura, T. *J. Am. Chem. Soc.* **1997**, *119*, 6284.
(18) Walker, F. A.; Simonis, U. Iron Porphyrin Chemistry. In *Encyclopedia of Inorganic Chemistry*; King, R. B., Ed.; Wiley & Sons Ltd.: Chichester, 1994; Vol. 4, pp 1785−1846.
(19) Safo, M. K.; Gupta, G. P.; Walker, F. A.; Scheidt, W. R. *J. Am. Chem. Soc.* **1991**, *113*, 5497.
(20) Safo, M. K.; Gupta, G. P.; Watson, C. T.; Simonis, U.; Walker, F. A.; Scheidt, W. R. *J. Am. Chem. Soc.* **1992**, *114*, 7066.
(21) Cheesman, M. R.; Walker, F. A. *J. Am. Chem. Soc.* **1996**, *118*, 7373.
(22) Shedbalkar, V. P.; Dugad, L. B.; Mazumdar, S.; Mitra, S. *Inorg. Chim. Acta* **1988**, *148*, 17.
(23) Van Caemelbecke, E.; Will, S.; Autret, M.; Adamian, V. A.; Lex, J.; Gisselbrecht, J. P.; Gross, M.; Vogel, E.; Kadish, K. M. *Inorg. Chem.* **1996**, *35*, 184.
(24) This work was presented at the 217th National Meeting of the American Chemical Society, Anaheim, CA, March 25, 1999.
(25) Evans, D. F. *J. Chem. Soc.* **1959**, 2003.
(26) Sur, S. K. *J. Magn. Reson.* **1989**, *82*, 169.

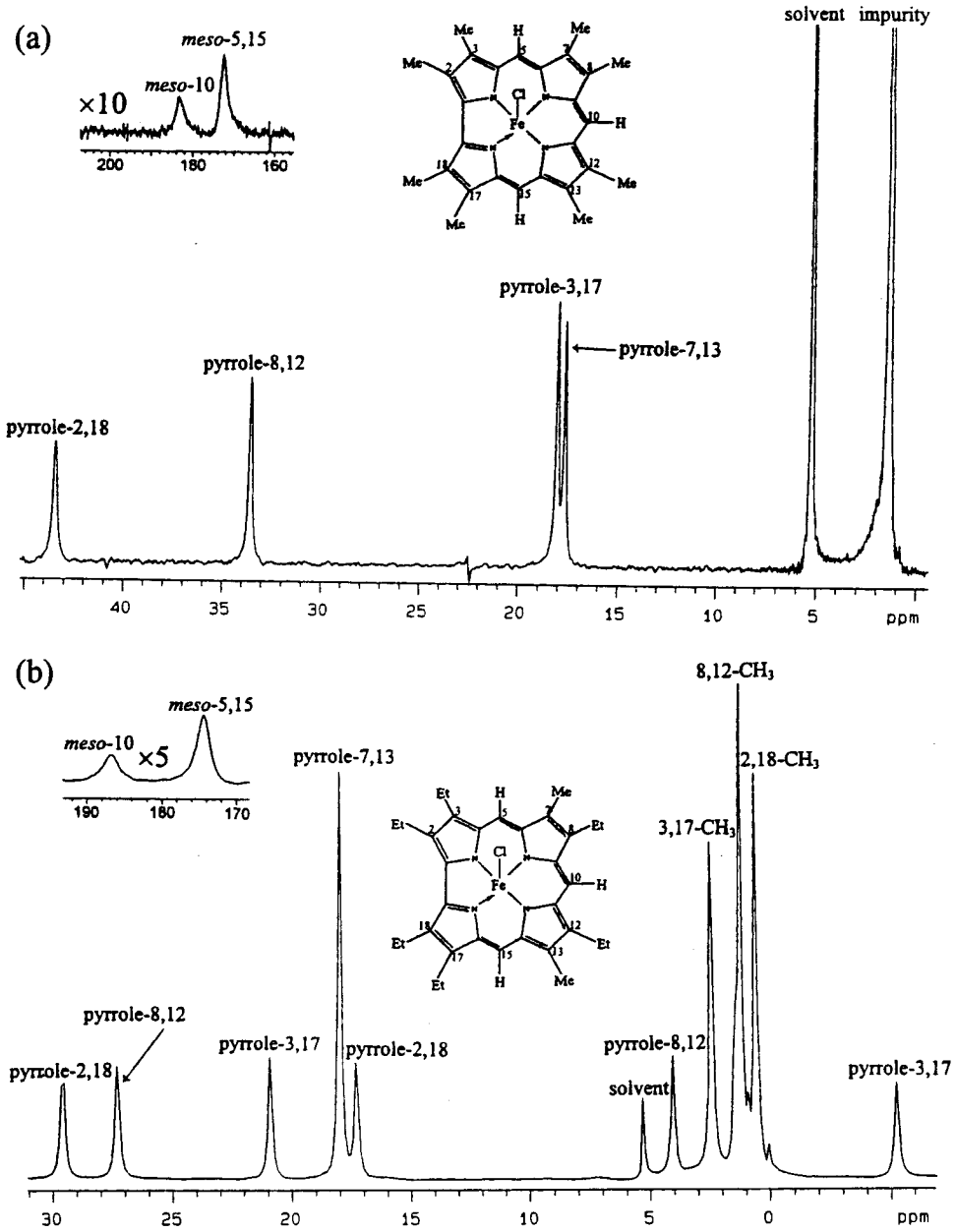

Figure 1. 1D spectra of (a) [(Me_8C)FeCl] and (b) [(7,13-Me_2Et_6C)FeCl] in CD_2Cl_2 at 30 °C, showing all methyl resonances and the strongly downfield-shifted *meso*-H resonances (insets), the latter expanded vertically by a factor of 5 or 10.

solvent, and *c* is the concentration (g/L) of the paramagnetic compound. The value of χ_M was calculated from χ in the usual way, and χ_M was corrected for the diamagnetic susceptibility of the corrole ligand, calculated from the sum of the Pascal constants.[27] The effective magnetic moment, μ_{eff}, was then calculated from χ_M(corr).

Results

[(Me_8C)FeCl] and [(7,13-Me_2Et_6C)FeCl]. In parts a and b of Figure 1 are shown the 1D spectra of [(Me_8C)FeCl] and [(7,13-Me_2Et_6C)FeCl] obtained at 30 °C, respectively. The COSY spectrum of [(7,13-Me_2Et_6C)FeCl] obtained at 30 °C is shown in Figure 2. The 1D and NOESY spectra of the latter complex obtained at −50 °C are shown in Figure S1 in the Supporting Information. The chemical shifts of [(Me_8C)FeCl] and [(7,13-Me_2Et_6C)FeCl] at 30 °C, together with the data for [(Et_8C)FeCl] taken from the literature,[8] are summarized in Table 1. The assignments are based on the COSY and NOESY spectra of [(7,13-Me_2Et_6C)FeCl], and by comparison of the chemical shifts of the three complexes. All resonances exhibit approximate Curie behavior, as shown in Figure 3 for the methyl and methylene resonances of the two complexes.

The NMR data demonstrate that [(7,13-Me_2Et_6C)FeCl] and [(Me_8C)FeCl] have the following properties: (a) both complexes have positive shifts for pyrrole CH_2 or CH_3 protons and very large positive shifts for the two types of *meso*-protons. (b) In [(7,13-Me_2Et_6C)FeCl], the two protons of each pyrrole CH_2 group are not magnetically equivalent because the mirror plane is lost due to the bound chloride. One of these protons has a negative or very small positive chemical shift, indicating a negative dipolar shift. (c) Substitution of methyl groups by ethyl groups at pyrrole positions results in a decrease of the chemical shift of the pyrrole alkyl protons. In fact, the methyl shifts of [(Me_8C)FeCl] are larger than the average methylene shifts of [(7,13-Me_2Et_6C)FeCl] by 87−130% (Table 1). Similar differ-

(27) Kahn, O. *Molecular Magnetism*; VCH Publishers: Weinheim, 1993; pp 2−4.

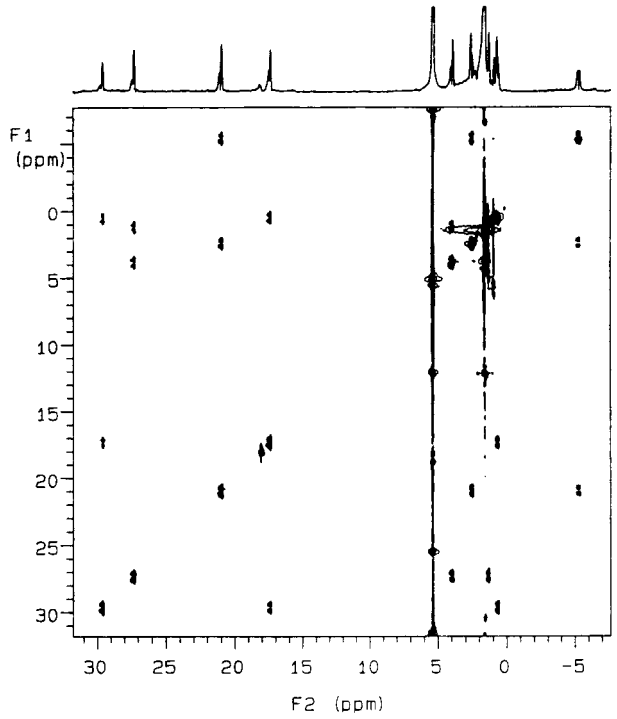

Figure 2. DQF-COSY spectrum of [(7,13-Me_2Et_6C)FeCl] at 30 °C. The diagonal projection is shown above the 2D spectrum, and hence the peak intensities are distorted with respect to those of Figure 1b. The cross-peaks in the DQF-COSY spectrum come from correlation of protons within ethyl groups. For each ethyl group, there are three pairs of cross-peaks: one from the correlation of the two protons of the CH_2 group and two from the correlation of the two CH_2 protons to the CH_3 protons.

ences in shifts are seen for methyls and methylenes in iron(III) porphyrins,[16,28] and are undoubtedly due to a combination of the difference in the number of protons to which spin is delocalized, as well as a preferred conformation for the methylene groups and thus a particular Karplus angle that affects the spin density at the methylene protons.

From the NOESY spectrum of [(7,13-Me_2Et_6C)FeCl], Figure S1, resonances from pyrrole 8,12-CH_2 and pyrrole 7,13-CH_3 can be assigned. Although the 2D data do not lead to assignment of which methylenes are at the 2,18 and 3,17 positions, a full assignment can be proposed by comparing the chemical shifts of this complex with those of [(Me_8C)Mn],[10] whose pyrrole groups have been completely assigned by systematic substitution. Since [(Me_8C)Mn] has the same number of valence electrons as [(Me_8C)FeCl] (see Table 2 and the Discussion) and they show similar ^{1}H NMR patterns, it is reasonable to conclude that they have the same order of pyrrole CH_3 shifts: pyrrole 2,18 > pyrrole 8,12 > pyrrole 3,17 > pyrrole 7,13 from the most downfield to the most upfield resonance. Because of the close spacing of the two methyl resonances near 18 ppm for [(Me_8C)FeCl] and the absence of corroborating information, the assignment of the 3,17 and 7,13 methyl signals is uncertain.

Both [(7,13-Me_2Et_6C)FeCl] and [(Me_8C)FeCl] are EPR silent. [(7,13-Me_2Et_6C)FeCl] shows an almost constant magnetic moment of 3.0 μ_B from 203 to 303 K, as shown in Figure 4a, indicating two unpaired electrons ($S = 1$) in this complex. The results are consistent with the magnetic moment of [(Et_8C)FeCl],[8] which is 2.97 μ_B at 293 K, measured by the Gouy method.

In Table 2 are summarized the chemical shifts of the alkyl substituents of the series of alkylcorrolate cation radical complexes of Mn(II) at 298 K in pyridine-d_5 reported previously,[10] as well as the same series of alkyl substituents for the corresponding neutral iron(III) complexes[29] (the one-electron-reduced products of the chloroiron(III) corrolate cation radicals discussed above, also in pyridine-d_5), together with those reported previously for the 1-electron-reduced complex [(Et_8C)Fe] in pyridine-d_5.[8] The neutral iron octaethylcorrolate has been shown to bind one pyridine,[8] and the same is true for the Mn corrolates, for which the room-temperature binding constant K_1 is 14.8 M^{-1} for pyridine binding to [(Me_8C)Mn] in chloroform.[10] Nevertheless, for both Mn and Fe neutral metal corrolates in pyridine-d_5 the two methylene protons of each ethyl group appear as a single resonance (Table 2). This is likely due to rapid exchange of bound and free pyridine out of and into the coordination sphere, above and below the metal. Consistent with this, Vogel and co-workers have reported that, in CS_2 in the absence of excess pyridine, the methylene protons of [(Et_8C)Fe(Py)] are not equivalent, and give rise to two separate resonances for each methylene group.[8] As can be seen from the data of Table 2, the pattern of shifts is similar for the neutral manganese and iron complexes, as well as those of the chloroiron corrole complexes presented in Table 1, except for the magnitudes of the shifts, which decrease in the order (R_8C)Fe > (R_8C)Mn > (R_8C)FeCl, and the magnitude and sign of the *meso*-H shifts, which are positive for (R_8C)Mn and (R_8C)FeCl and negative for the neutral Fe corrolates. These *meso*-H shifts support the conclusion, considered further in the Discussion, that the iron(III) corrolates are simple $S = 3/2$ Fe(III) complexes while the manganese and chloroiron corrolates are $S = 3/2$ Mn(II) and $S = 3/2$ Fe(III), respectively, each coupled antiferromagnetically to a (corrolate)$^{2-}$ radical. In support of this conclusion, the magnetic moment of the 1-electron-reduced iron octaethylcorrolate bound to one pyridine molecule is consistent with $S = 3/2$,[8] while the manganese pyridine[10] and chloroiron (this work) corrolates both have magnetic moments that are consistent with an overall $S = 1$.

[(Me_8C)FeCl] and [(7,13-Me_2Et_6C)FeCl] in the Presence of Axial Imidazole Ligands. If an excess of axial ligand (either imidazole or *N*-methylimidazole) is present in the solution of [(Me_8C)FeCl] or [(7,13-Me_2Et_6C)FeCl], several tiny peaks can be seen in their proton NMR spectra at room temperature, Figure 5a, which may arise from both mono- and bisimidazole complexes. Low temperature favors the binding of imidazole, and below −50 °C, only bisimidazole complexes are present in the solution, Figure 5b,c. In the spectrum of [(7,13-Me_2Et_6C)FeCl] with axial ligands at −70 °C, only three pyrrole α-CH_2 resonances of relative area 4 are shown instead of six peaks of relative area 2, as shown in free [(7,13-Me_2Et_6C)FeCl]. This, as well as the integrated intensities of the coordinated imidazole peaks, demonstrates that the iron centers have two imidazole ligands bound, so that the two CH_2 protons of each pyrrole ethyl group are now magnetically equivalent. Bisimidazole complexes [(Me_8C)Fe($L)_2$]$^+$Cl$^-$ and [(7,13-Me_2Et_6C)Fe($L)_2$]$^+$Cl$^-$ (L = imidazole or *N*-methylimidazole) exist only at low temperatures. With increasing temperature, the complexes dissociate into [(7,13-Me_2Et_6C)Fe(L)Cl] or [(Me_8C)Fe(L)Cl] (or their Cl$^-$-dissociated forms), and finally, at room temperature, are nearly completely in the 5-coordinate [(7,13-Me_2Et_6C)FeCl] or [(Me_8C)FeCl] form.

To simplify the spectra of the bisimidazole complexes, deuterated imidazole (Im-d_4) was used as axial ligand. In the

(28) Caughey, W. S.; Johnson, L. F. *J. Chem. Soc., Chem. Commun.* **1969**, 1362.

(29) Licoccia, S. Unpublished work.

Table 1. ^{1}H Chemical Shifts (ppm) and Assignments of Chloroiron Alkylcorrolates at 300 K

[(Me_8C)FeCl][a]	[(7,13-Me_2Et_6C)FeCl][a]	[(Et_8C)FeCl][8,b]	assignment
183 (1H)	187 (1H)	189 (1H)	*meso*-10
172 (2H)	174 (2H)	177 (2H)	*meso*-5,15
43.7 (6H)	29.7 (2H)	29.2 (2H)	pyrrole 2,18-CH_2 or -CH_3[c]
	17.3 (2H)	17.7 (2H)	
33.8 (6H)	27.3 (2H)	27.8 (2H)	pyrrole 8,12-CH_2 or -CH_3
	4.1 (2H)	3.7 (2H)	
18.2 (6H)	20.9 (2H)	21.3 (2H)	pyrrole 3,17-CH_2 or -CH_3[c]
	−5.2 (2H)	−5.7 (2H)	
18.0 (6H)	18.0 (6H)	15.8 (2H)	pyrrole 7,13-CH_2 or -CH_3
		0.0 (2H)	
	2.5 (6H)	2.5 (6H)	CH_2CH_3-3,17[c]
	1.2 (6H)	1.3 (6H)	CH_2CH_3-8,12
	0.6 (6H)	0.6 (6H)	CH_2CH_3-2,18[c]
		−0.3 (6H)	CH_2CH_3-7,13

[a] This work. [b] Assignments not reported; assignments listed are based upon those for [(3,17-Me_2Et_6C)FeCl]. [c] Assignments based upon comparison to the "Mn(III) corrolate" assignments (actually manganese(II) corrolate cation radical; see Table 2).[10]

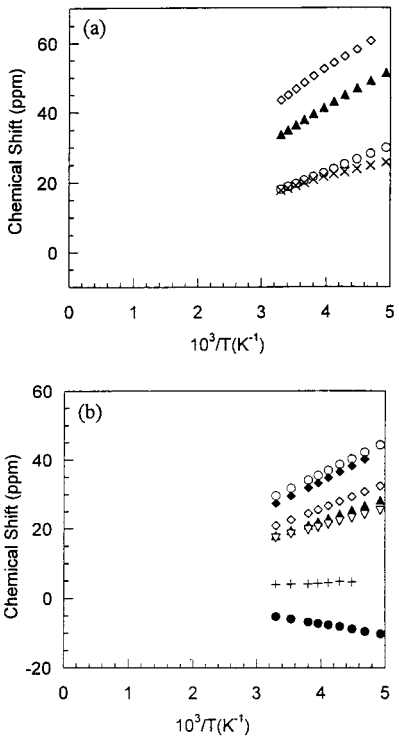

Figure 3. Curie plot of the pyrrole substituent resonances of (a) [(Me_8C)FeCl] and (b) [(7,13-Me_2Et_6C)FeCl]. Solvent = CD_2Cl_2. Symbols: (a) ◇, 2,18-CH_3; ▲, 8,12-CH_3; ○, 3,17-CH_3; ×, 7,13-CH_3; (b) ○, 2,18-CH_2; ◆, 8,12-CH_2; ◇, 3,17-CH_2; ▲, 7,13-CH_3; ▽, 2,18-CH_2; +, 8,12-CH_2; ●, 3,17-CH_2; based upon the assignments given in Table 1 (see the text).

1D spectrum of [(7,13-Me_2Et_6C)Fe(Im-d_4)$_2$]$^+$Cl$^-$, there is one more peak in addition to pyrrole, *meso*-H, and solvent signals, as shown in Figure 5c. This resonance arises from the ligand N−H. Since there may have been traces of H_2O present in the solution, the N−D of Im-d_4 probably exchanged with H_2O to produce N−H. When a drop of D_2O was added to the solution, the N−H peak of the coordinated imidazole disappeared.

As in the cases of [(7,13-Me_2Et_6C)FeCl] and [(Me_8C)FeCl], partial assignments can be made from the 2D spectra of the imidazole complexes, as shown in Figure 6 and its caption, and relative peak areas. Furthermore, if the number of equivalents of imidazole added to the chloroiron corrolate is less than two, or the temperature is above −50 °C, then peaks from both chloroiron starting material and the bisimidazole complex, and even tiny peaks from the monoimidazole complex, can be observed in the 1D spectra, as shown in Figure 5a. To make full assignments of the bisimidazole complexes, EXSY spectra were recorded at 243 K. The spectra show the chemical exchange between the chloroiron starting material and the bisimidazole complex, as shown in Figure 7. Below 243 K, EXSY spectra instead show chemical exchange between the mono- and bisimidazole complexes, as shown in Figure 10.

In the EXSY spectrum of Figure 7, recorded at 243 K, there are cross-peaks between the 5-coordinate chloroiron complex 2,18-CH_2 resonances at 36 and 21 ppm and the broad peak at −12 ppm, between the chloroiron 8,12-CH_2 resonances at 34 and 2 ppm and the broad peak at 13 ppm, between the chloroiron 3,17-CH_2 resonances at 26 and −8 ppm and the broad peak at 39.5 ppm, and between the chloroiron 7,13-CH_3 peak at 22 ppm and the broad peak at −9 ppm. Thus, on the basis of the assignment of the resonances of [(7,13-Me_2Et_6C)FeCl], Tables 1, 2, the chemical shift order for [(7,13-Me_2Et_6C)Fe(ImH)$_2$]Cl is pyrrole 3,17 > pyrrole 8,12 > pyrrole 7,13 > pyrrole 2,18 from the most downfield to the most upfield resonance. Simple Hückel molecular orbital calculations[16] predict this order as well, assuming that the unpaired electrons on the metal and the corrole rings are either uncoupled or weakly ferromagnetically coupled, although the chemical shifts predicted on this basis are larger than observed. This might suggest that the coupling pathway is instead weakly antiferromagnetic in nature. Higher-level molecular orbital calculations would be required to unambiguously delineate the coupling pathway. The chemical shifts and assignments for the bisimidazole complexes at 203 K are listed in Table 3.

In contrast to [(7,13-Me_2Et_6C)FeCl] and [(Me_8C)FeCl], the bisimidazole complexes have large *upfield* shifts for the *meso*-H resonances, Figure 5b,c. This implies that the 5-coordinate chloride compounds and their bisimidazole complexes have different electronic structures. The Curie plots of these bisimidazole complexes also show more complicated behavior, as shown in Figure 8. If the imidazole:5-coordinate chloride compound ratio is not very high (on the order of 5:1), both the *meso*-H and pyrrole CH_2 or CH_3 resonances show anti-Curie behavior. These resonances shift with a change in concentration of imidazole or chloroiron corrolate, indicating the presence of a chemical equilibrium. Upon doubling the imidazole concentration, the temperature dependence of the resonances becomes less anti-Curie in nature (Figure 8b). Upon diluting the chloroiron corrolate while keeping the concentration of imidazole constant, the temperature dependence of the *meso*-H changes from weakly anti-Curie to weakly Curie in nature (Figure 8c); however, the intercepts of all of these plots are quite negative

Table 2. ^{1}H Chemical Shifts (ppm) and Assignments of Manganese Alkylcorrolates at 298 K,[10] as Compared to Those of the Neutral Iron(III) Alkylcorrolates,[8,29] Also at 298 K

[(R$_8$C)Mn] in pyridine-d_5[10]	[(R$_8$C)Fe^{III}] in pyridine-d_5[29]	[(Et$_8$C)Fe^{III}] in pyridine-d_5[8]	assignment
25.0 (1H)	−62.2 (1H)	−62.2 (1H)	*meso*-10
70.5 (2H)	−16.0 (2H)	−15.9 (2H)	*meso*-5,15
112.4 (6H)	131.1 (6H)		pyrrole 2,18-CH_3
64.3 (6H)	75.0 (6H)		pyrrole 8,12-CH_3
45.5 (6H)	56.4 (6H)		pyrrole 3,17-CH_3
15.8 (6H)	14.1 (6H)		pyrrole 7,13-CH_3
55.0 (4H)	66.5 (4H)	67.7 (4H)	pyrrole 2,18-CH_2
35.6 (4H)	38.2 (4H)	37.9 (4H)	pyrrole 8,12-CH_2
21.5 (4H)	27.2 (4H)	28.5 (4H)	pyrrole 3,17-CH_2
−8 (4H)		1.9 (4H)	pyrrole 7,13-CH_2
−123.0 (2H)			pyrrole 2,18-*H*
−40.0 (2H)			pyrrole 3,17-*H*

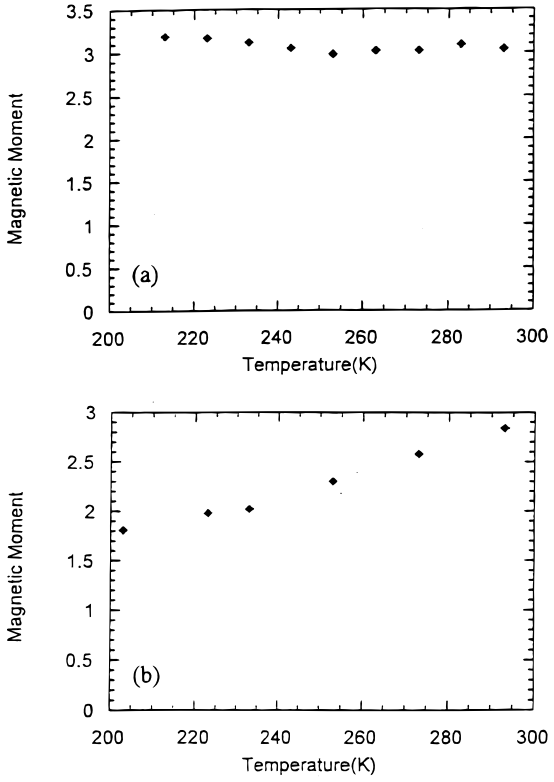

Figure 4. Magnetic moment in CD_2Cl_2 as a function of temperature for [(7,13-Me$_2$Et$_6$C)FeCl]: (a) without imidazole ligands and (b) the bis-*N*-methylimidazole complex.

compared to the diamagnetic shifts of the corrole *meso*-H. The concentration dependence of both imidazole and chloroiron corrolate indicates that the bisimidazole complex is not very stable and is in reasonably fast chemical exchange with the monoimidazole complex at higher temperatures, and it is not possible to increase the concentration of imidazole high enough to fully form the bisimidazole complex at all but the very lowest temperatures investigated (down to 183 K). Thus, the chemical shifts listed in Table 3 must be considered only approximate.

The calculated magnetic moment of the bisimidazole complex of [(7,13-Me$_2$Et$_6$C)FeCl] was found to decrease with decreasing temperature, with $\mu_{eff} = 2.8\ \mu_B$ at 293 K, 2.3 μ_B at 253 K, 1.95 μ_B at 223 K, and 1.8 μ_B at 203 K, as shown in Figure 3b. Above 250 K, the temperature dependence is probably due to the presence of the chloroiron complex as well as the mono- and bisimidazole complexes, while a value of 2.6 μ_B would suggest two unpaired electrons having uncoupled spins,[30] and 1.8 μ_B suggests one unpaired electron. Initially it was thought that these results indicated a low-spin Fe(III) center ferromagnetically coupled to a corrolate cation radical, which then formed a dimer at low temperatures in which the corrole cation radicals were coupled to cancel the spin on the macrocycle. However, this explanation is inconsistent with the NMR data discussed above and below. Instead, it must be pointed out that the magnetic moment, calculated from the magnetic susceptibility measured

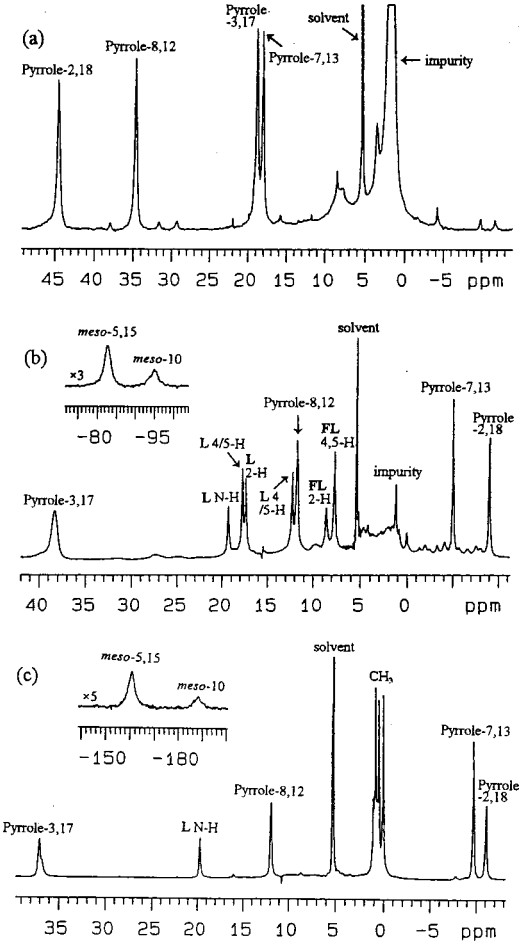

Figure 5. 1D spectra of (a) [(Me$_8$C)FeCl] with imidazole-d_4 in CD_2Cl_2 at 20 °C with a spectral width of 16 kHz, (b) [(Me$_8$C)Fe(Im-h_4)$_2$]Cl at −70 °C, and (c) [(7,13-Me$_2$Et$_6$C)Fe(Im-d_4)$_2$]Cl at −70 °C. The assignments were made from 2D spectra (see Figure 5). *N*-Methylimidazole complexes show almost the same spectra, except that the N−H is replaced by a methyl group and the binding of two axial ligands requires lower temperatures. Peaks marked L are due to bound imidazole ligands, and FL stands for free imidazole. The *meso*-H resonances, which are shifted strongly upfield, are shown in the insets of (b) and (c).

(30) Kahn, O. *Molecular Magnetism*, VCH Publishers: Weinheim, 1993; pp 103−132.

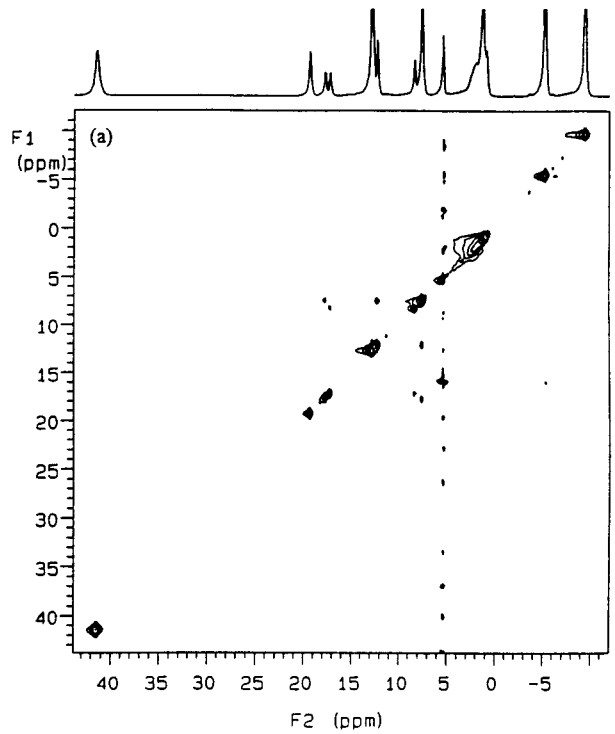

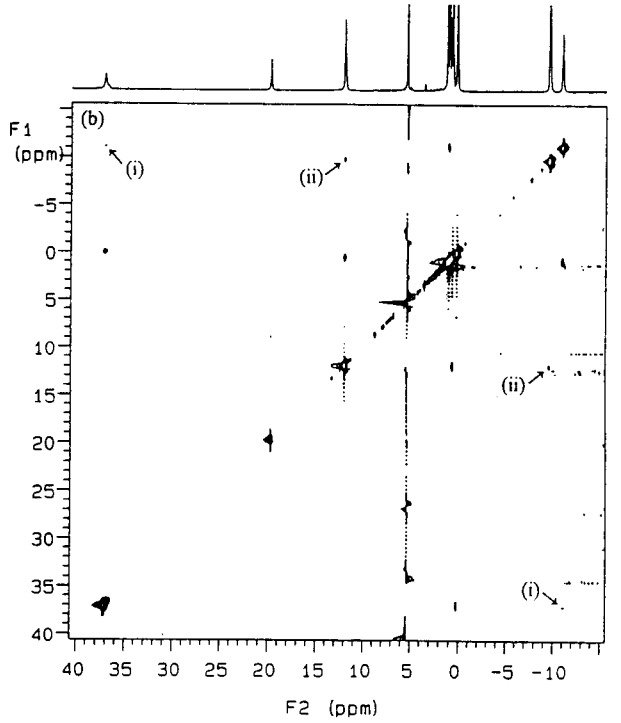

Figure 6. (a) NOESY spectrum of $[(Me_8C)Fe(Im\text{-}h_4)_2]Cl$ in CD_2Cl_2 at −60 °C. All cross-peaks are from chemical exchange between free and bound imidazole. Partial assignments of the imidazole ligand protons have been made. (b) NOESY spectrum of $[(7,13\text{-}Me_2Et_6C)Fe(Im\text{-}d_4)_2]Cl$ at −70 °C. Unlike the $[(Me_8C)Fe(Im\text{-}d_4)_2]Cl$ complex, $[(7,13\text{-}Me_2Et_6C)Fe(Im\text{-}d_4)_2]Cl$ is soluble enough to allow detection of weak NOE cross-peaks. Two pairs of cross-peaks are shown here: (i) between pyrrole 2,18-CH_2 protons and pyrrole 3,17-CH_2 protons and (ii) between pyrrole 7,13-CH_3 protons and pyrrole 8,12-CH_2 protons.

by the Evans method,[25,26] assumes that the concentration of the complex is known at each temperature. This is not the case for the bisimidazole complexes, which are very insoluble and visibly precipitate at low temperatures. Hence, the decrease in magnetic

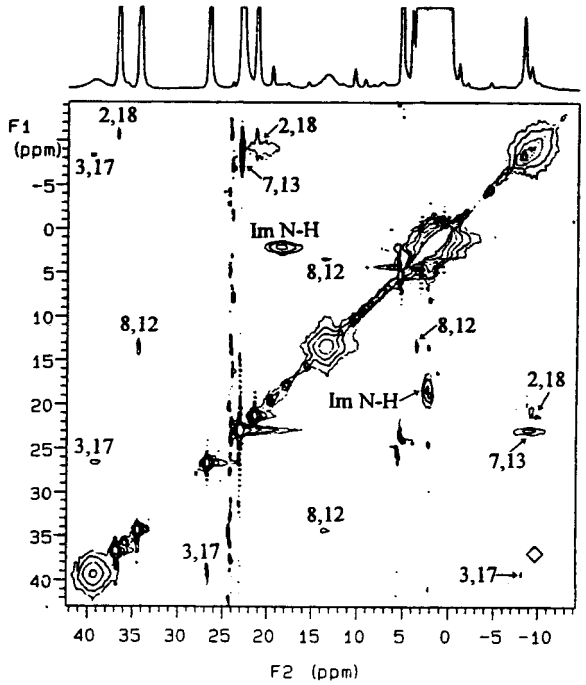

Figure 7. NOESY/EXSY spectrum of a mixture of $[(7,13\text{-}Me_2Et_6C)FeCl]$ and $[(7,13\text{-}Me_2Et_6C)Fe(ImH)_2]^+Cl^-$, recorded at 243 K in CD_2Cl_2. The resonances of the 3,17-CH_2 protons at 26.5 and −8.5 ppm that are due to the chloroiron complex are in chemical exchange with the broad peak of the bisimidazole complex at 39 ppm, the resonances of the 2,18-CH_2 protons at 36 and 21.5 ppm that are due to the chloroiron complex are in chemical exchange with a broad, unresolved peak of the bisimidazole complex at −10 ppm, the resonances of the 8,12-CH_2 protons at 34 and 3.7 ppm that are due to the chloroiron form are in chemical exchange with the broad peak of the bisimidazole complex at 13 ppm, and the resonance of the 7,13-CH_3 protons at 23 ppm that is due to the chloroiron form is in chemical exchange with the peak of the bisimidazole complex at −9 ppm. The position of the cross-peak below the diagonal between the 2,18-CH_2 resonance of the chloroiron complex at 36 ppm and the bisimidazole complex at −10 ppm that is too weak to be observed at the contour level of this plot is shown by the tilted square symbol. Strong chemical exchange cross-peaks are also observed between the N−H resonances of the free imidazole at 2 ppm and the bound imidazole of the bisimidazole complex at 17.5 ppm.

moment as the temperature is lowered is probably due to formation of crystallites of the complex, because this precipitation of the complex would lower the concentration of the complex in solution, which would give rise to a smaller frequency shift of the signal used for measuring the magnetic susceptibility,[25,26] hence leading to a smaller calculated magnetic moment if the concentration of the complex in solution is assumed constant. Because of the low solubility of the complex, an accurate magnetic susceptibility would need to be measured at very low concentrations, but at these low concentrations the frequency shift[25,26] is extremely small, leading to low accuracy of the calculated magnetic moment. Thus, the magnetic moment data are not very useful in determining the overall spin of the complex and the possible coupling mode of the unpaired electrons.

The EPR spectrum of $[(Me_8C)Fe(ImH)_2]^+Cl^-$ is shown in Figure 9 and indicates a low-spin Fe(III) center, with no evidence of the macrocycle unpaired electron. The g values of $[(7,13\text{-}Me_2Et_6C)Fe(ImH)_2]^+Cl^-$ are essentially identical ($g_1 = 2.56$, $g_2 = 2.21$, $g_3 = 1.83$) to those of the octamethylcorrolate complex. Quantitative comparison of the integrated intensity of the $[(7,13\text{-}Me_2Et_6C)Fe(ImH)_2]^+Cl^-$ signal to that of a similar rhombic low-spin Fe(III) EPR spectrum, that of [(TMP)-

Table 3. ^{1}H Chemical Shifts (ppm) and Assignments of the Bisimidazole Complexes of the Chloroiron Alkylcorrolates, Formed in the Presence of ~15 mM Imidazole at 203 K

$[(Me_8C)Fe(ImH)_2]Cl$[a]	$[(7,13\text{-}Me_2Et_6C)Fe(ImH)_2]Cl$[b]	assignment
−95.1 (1H)	−188.5 (1H)	*meso*-10
−82.8 (2H)	−161.3 (2H)	*meso*-5,15
38.2 (6H)	37.1 (4H)	pyrrole 3,17-CH_2 or -CH_3
11.7 (6H)	11.9 (4H)	pyrrole 8,12-CH_2 or -CH_3
−5.0 (6H)	−9.7 (6H)	pyrrole 7,13-CH_3
−9.1 (6H)	−11.1 (4H)	pyrrole 2,18-CH_2 or -CH_3

[a] Concentration <1 mM. [b] Concentration ~4 mM.

Table 4. ^{1}H Chemical Shifts (ppm) and Assignments of the Monoimidazole Complexes of the Chloroiron Alkylcorrolates, Formed in the Presence of ~15 mM Imidazole

$[(Me_8C)Fe(ImH)Cl]$[a] or $[(Me_8C)Fe(ImH)]^+Cl^-$	$[(7,13\text{-}Me_2Et_6C)Fe(ImH)Cl]$[b] or $[(7,13\text{-}Me_2Et_6C)Fe(ImH)]^+Cl^-$	assignment
		meso-10
		meso-5,15
68.0 (6H)	45.1, 28.6 (2H, 2H)	pyrrole 2,18-CH_2 or -CH_3
63.6 (6H)	46.6, 5.4 (2H, 2H)	pyrrole 3,17-CH_2 or -CH_3
21.7 (6H)	23.4 (6H)	pyrrole 7,13-CH_3
76.9 (6H)	53.1, 17.0 (2H, 2H)	pyrrole 8,12-CH_2 or -CH_3

[a] Recorded at 218 K; concentration <1 mM. [b] Recorded at 213 K; concentration ~4 mM.

$Fe(ImH)_2]^+Cl^-$, both at 1 mM concentration, showed that the ratio of intensities was about 0.6:1. Hence, the rhombic EPR signals of $[(Me_2Et_6C)Fe(ImH)_2]^+Cl^-$ and its octamethylcorrole counterpart are certainly not those of small impurities, and in fact, the approximate factor of 2 difference in signal intensity is consistent with partial precipitation (formation of tiny crystallites whose EPR signals are sharply attenuated due to exchange between unpaired electrons that are separated by less than about 10−12 Å) by $[(Me_2Et_6C)Fe(ImH)_2]^+Cl^-$ or its octamethyl counterpart as they are frozen. The intensity of the signal between 4.2 and 25 K increases approximately according to Curie law, and it is not readily saturated over the microwave power attenuation range of 50−20 dB.

Although the NMR resonances of the monoimidazole complex of $[(7,13\text{-}Me_2Et_6C)FeCl]$ are extremely small in the 1D spectra (Figure 5a), their chemical shifts can be measured and peak assignments can be made on the basis of EXSY spectra that show the chemical exchange between the mono- and bisimidazole complexes, as shown in Figure 10. Table 4 lists the chemical shifts and assignments of the pyrrole CH_2 and CH_3 resonances. Since no information was obtained on the positions of the *meso*-H resonances, and since the order of alkyl resonances (8 > 2 > 3 ≫ 7) differs from that found for both the chloroiron (2 > 8 ≫ 3 > 7) and bisimidazole (3 ≫ 8 > 7 > 2) complexes, the electronic structure of the monoimidazole complexes is still unknown.

Discussion

Electronic Structure of $[(Me_8C)FeCl]$ and $[(7,13\text{-}Me_2Et_6C)FeCl]$. The large downfield shifts of the *meso*-H resonances of these complexes (Figure 1) are striking. Usually, $d_{x^2-y^2}$ is the highest energy d orbital of the metal center in a metal tetrapyrrole complex,[14,16] and for an intermediate spin ($S = 3/2$) complex, it is thus empty. Thus, there should be little σ spin delocalization at the *meso* positions in $[(Me_8C)FeCl]$, and even if there were an unpaired electron in the $d_{x^2-y^2}$ orbital, it could not cause large *downfield* shifts (to nearly 200 ppm). Such large downfield shifts of *meso*-H resonances can only arise from very large negative π spin delocalization, and then only when there is an unpaired electron, which has a spin opposite that in the metal center, in the corrole ring. Even larger positive chemical shifts have been reported for iron(III) octaethyloxophlorin π cation radicals.[31] In this case, however, the electron configuration is high-spin Fe(III) ($S = 5/2$), rather than intermediate-spin Fe(III) ($S = 3/2$), coupled to a porphyrin π cation radical with a_{2u} symmetry, and thus producing very large spin density at the *meso* positions. Although the chloroiron corrolate complex of this study is $S = 3/2$, the same a_{2u}-type symmetry of the HOMO of the corrole can certainly lead to antiferromagnetic coupling of the corrolate radical electron with the $S = 3/2$ Fe(III). Similar antiferromagnetic coupling of the porphyrinate radical electron with an $S = 3/2$, 5/2 spin-admixed Fe(III) was found to be consistent with the Mössbauer quadrupole splitting and temperature dependence of the magnetic susceptibility for $[(OEP)Fe(ClO_4)_2]$,[32] for which the average Fe−N bond length is 1.999(2) Å. In contrast, the Fe−N bond lengths of the iron(III) octaethyloxophlorin π cation radical are much longer (2.07 Å)[31] than those of the Fe−N bond lengths of the iron(III) octaethylporphyrin π cation radical[32] or the chloroiron corrolate (1.91 Å),[8] consistent with a shift to higher energy and thus the depopulation of the $d_{x^2-y^2}$ orbital in the iron corrolate $S = 3/2$ π cation radical complex.

As a result, it can be concluded that, at least for the chloroiron complexes, the so-called iron(IV) corrolates[8] are actually iron(III) corrolate π cation radicals. The intermediate-spin Fe(III) center ($S = 3/2$) and the corrole ring unpaired electron are antiferromagnetically coupled, giving a net spin $S = 1$, as measured. From the methods utilized in the present and previous[8,11,23] work, it is not possible to determine whether there may be some $S = 3/2$, 5/2 spin admixture. Although the 2,18 and 3,17 pyrrole substituent shifts cannot be unambiguously assigned on the basis of the two complexes studied, it is reasonable that the pyrrole CH_3 shifts are in the same order as those of the manganese(II) corrolate cation radical complexes listed in Table 2:[10] pyrrole 2,18 > pyrrole 8,12 > pyrrole 3,17 > pyrrole 7,13 from the most downfield to the most upfield resonance.

(31) Balch, A. L.; Latos-Grazynski, L.; Noll, B. C.; Szterenberg, L.; Zovinka, E. P. *J. Am. Chem. Soc.* **1993**, *115*, 11846.

(32) Scheidt, W. R.; Song, H.; Haller, K. J.; Safo, M. K.; Orosz, R. D.; Reed, C. A.; Debrunner, P. G.; Schulz, C. E. *Inorg. Chem.* **1992**, *31*, 941.

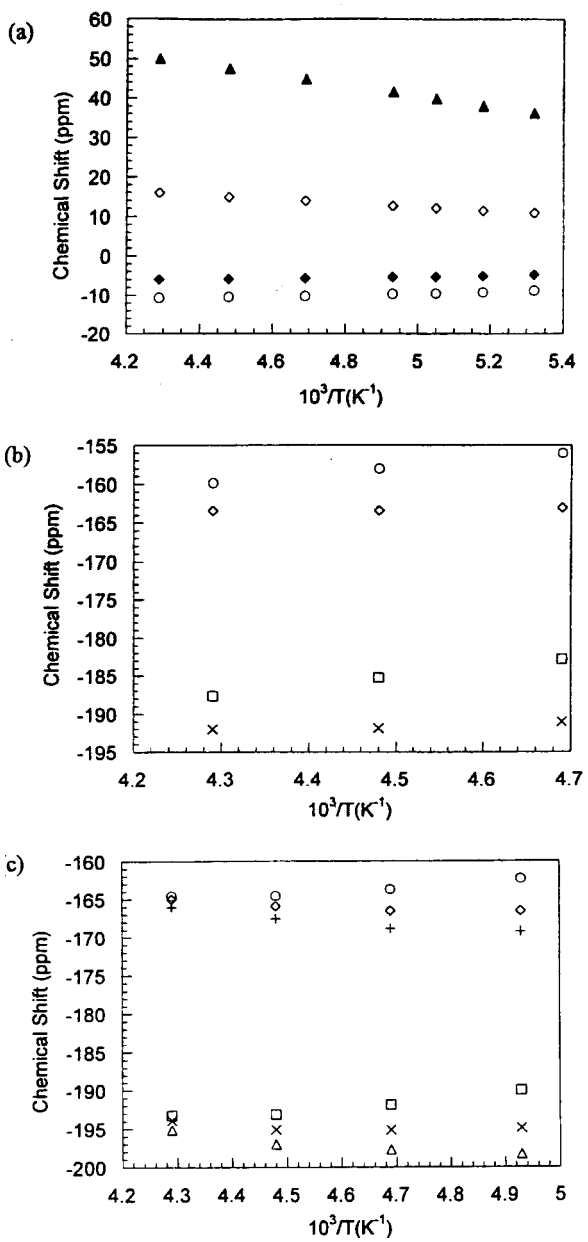

Figure 8. Curie plot of (a) $[(Me_8C)Fe(Im\text{-}d_4)]^+Cl^-$ CH_3 resonances, showing non-Curie behavior (solvent = CD_2Cl_2), (b) $[(7,13\text{-}Me_2\text{-}Et_6C)Fe(ImH)_2]^+Cl^-$ *meso*-H resonances (solvent = CD_2Cl_2) (○, ◇, 5,15-H; □, ×, 10-H; ○, □, [ImH] ≈ 20 mM; ◇, ×, [ImH] ≈ 40 mM; concentration of $[(Me_2Et_6C)FeCl]$ ≈ 4 mM, constant for the two samples), and (c) $[(7,13\text{-}Me_2Et_6C)Fe(ImH)_2]^+Cl^-$ *meso*-H resonances (solvent = CD_2Cl_2) (○, ◇, +, 5,15-H; □, ×, △, 10-H; ○, □, total concentration of $[(Me_2Et_6C)FeCl]$ ≈ 4 mM; ◇, ×, total concentration of $[(Me_2Et_6C)FeCl]$ ≈ 2 mM; +, △, total concentration of $[(Me_2Et_6C)$-FeCl] ≈ 1 mM). The concentration of imidazole is constant in all three samples.

The unpaired electron of the corrole ring must be in the $7b_1$ orbital,[33] which has large density at the *meso* positions, similar to that of the a_{2u} orbital of the related porphyrin macrocycle,[16] and thus results in large negative π spin density on the *meso*-carbons and large downfield shifts of the *meso*-H resonances. Interestingly, simple Hückel calculations suggest that the $7b_1$ orbital is higher in energy than the metal d_{xz} and d_{yz} orbitals.[16] The strong antiferromagnetic coupling of the corrolate unpaired electron with the $S = 3/2$ iron(III) probably causes fast electronic

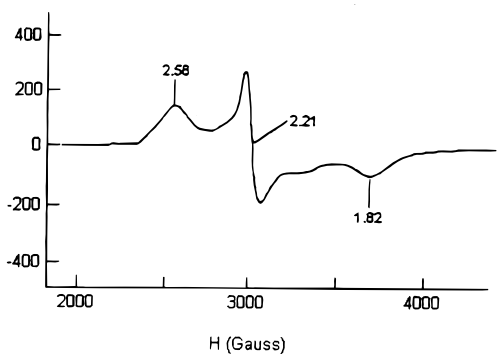

Figure 9. EPR spectrum of $[(Me_8C)Fe(ImH)_2]Cl$ in CD_2Cl_2 at 4.2 K (microwave frequency 9.341 GHz, microwave power 0.2 mW, modulation frequency 100 kHz, modulation amplitude 2 G).

relaxation of the iron center, so that no signal can be observed in the EPR spectra. That the antiferromagnetic coupling is strong is confirmed by the near-Curie temperature dependence of the proton resonances, Figure 3.

In fact, π cation radicals are common for both transition-metal porphyrinates and corrolates. The monopyridine complexes of manganese alkylcorrolates mentioned above, which have similar ^1H NMR patterns, were shown to be the valence tautomer $[(Me_8C^{\bullet 2-})Mn^{II}Py]$, in which the Mn(II) is in the $S = 3/2$ state and the corrole unpaired electron is antiferromagnetically coupled to the metal electrons.[10] The fact that substitution of pyrrole methyl groups by protons leads to reversal of the sign of the chemical shifts[10] indicates that contact shifts from π spin delocalization dominate the chemical shifts at these positions. We expect the same case in the chloroiron corrolates. However, the shifts of the *meso*-H of $[(Me_8C)Mn]$ (Table 2) are upfield as compared to those of $[(Me_8C)FeCl]$ (Table 1), while the shifts of pyrrole methyl protons are downfield as compared to those of $[(Me_8C)FeCl]$. This can be tentatively attributed to much stronger antiferromagnetic coupling in the iron case, which results in less positive spin density at the pyrrole positions and more negative spin density at the *meso* positions.

The assignment of an iron(IV) center in the complex $[(Et_8C)$-FeCl] has previously been supported by the reported zero-field Mössbauer parameters.[8,23] In Table 5 are listed Mössbauer parameters of some $S = 3/2$ Fe(III) and $S = 1$ Fe(IV) complexes from the literature. Fe(IV) centers are seen to have quite variable values of ΔE_Q, which range from 1.26 to 1.56 mm/s for ferryl systems[34−36] to 2.12 mm/s for $[(TMP)Fe(OCH_3)_2]$,[37] but a much larger value of 3.38 mm/s for a 6-coordinate non-porphyrin ligand complex.[38] The isomer shifts of these complexes range from 0.1 mm/s for the ferryl systems[34] to −0.03 mm/s for the bismethoxy tetramesitylporphyrinate complex[37] to −0.04 mm/s for the 6-coordinate non-porphyrin ligand complex.[38] In com-

(33) Hush, N. S.; Dyke, J. M.; Williams, M. L.; Woolsey, I. S. *J. Chem. Soc., Dalton Trans.* **1974**, 395.

(34) Simonneaux, G.; Sholz, W. F.; Reed, C. A.; Lang, G. *Biochim. Biophys. Acta* **1982**, *716*, 1.
(35) Boso, B.; Lang, G.; McMurry, T. J.; Groves, J. T. *J. Chem. Phys.* **1983**, *79*, 1122.
(36) Groves, J. T.; Gilbert, J. A. *Inorg. Chem.* **1986**, *25*, 123.
(37) Groves, J. T.; Quinn, R.; McMurry, T. J.; Nakamura, M.; Lang, G.; Boso, B. *J. Am. Chem.* Soc. **1985**, *107*, 354.
(38) Collins, T. J.; Fox, B. G.; Hu, Z. G.; Kostka, K. L.; Mhnck, E.; Rickard, C. E. F.; Wright, L. J. *J. Am. Chem. Soc.* **1992**, *114*, 8724.
(39) Dolphin, D. H.; Sams, J. R.; Tsin, T. B. *Inorg. Chem.* **1977**, *16*, 711.
(40) Masuda, H.; Taga, T.; Osaki, K.; Sugimoto, H.; Yoshida, Z.; Ogoshi, H. *Bull. Chem. Soc. Jpn.* **1982**, *55*, 3891.
(41) Gupta, G. P.; Lang, G.; Scheidt, W. R.; Geiger, D. K.; Reed, C. A. *J. Chem. Phys.* **1986**, *85*, 5212.
(42) Gismelseed, A.; Bominaar, E. L.; Bill, E.; Trautwein, A. X.; Winkler, H.; Nasri, H.; Doppelt, P.; Mandon, D.; Fischer, J.; Weiss, R. *Inorg. Chem.* **1990**, *29*, 2741.

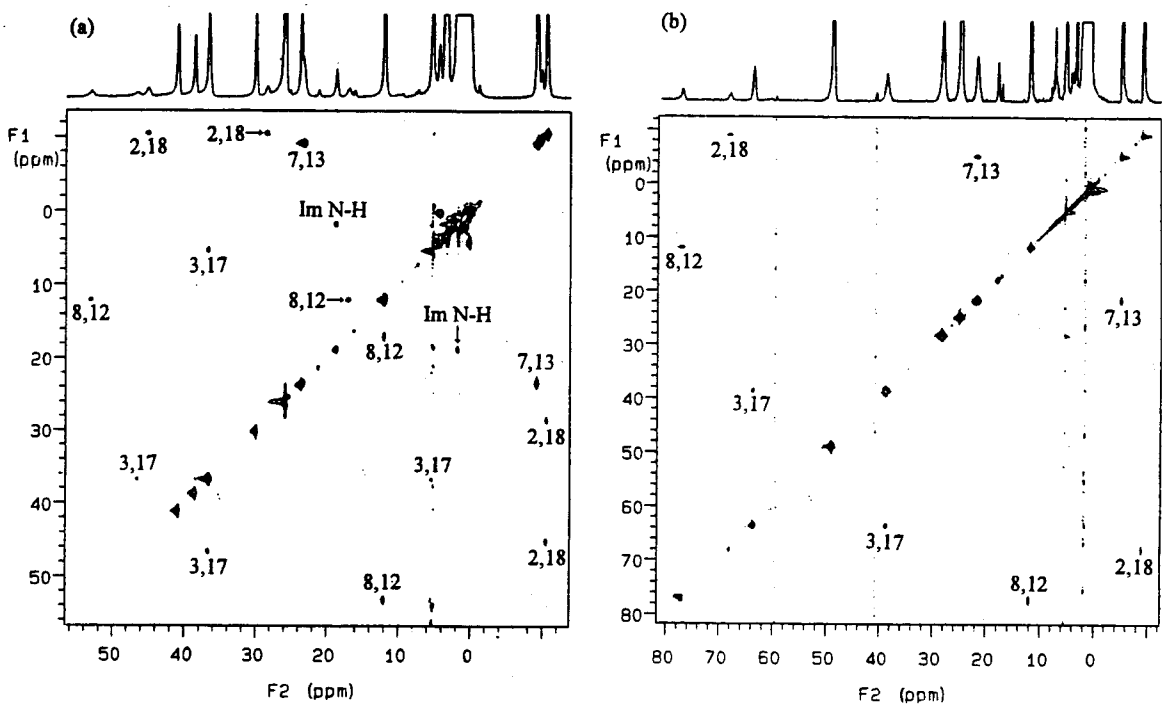

Figure 10. (a) EXSY spectrum of a mixture of [(7,13-Me_2Et_6C)FeCl] and its mono- and bisimidazole complexes recorded at 213 K in CD_2Cl_2. At this temperature, chemical exchange cross-peaks are observed only between the mono- and bisimidazole complexes. The 3,17-CH_2 resonance of the bisimidazole complex at 36.5 ppm gives chemical exchange cross-peaks to the tiny monoimidazole complex peaks at 46.5 and buried at 5 ppm, the 8,12-CH_2 resonance of the bisimidazole complex at 12 ppm gives chemical exchange cross-peaks to the tiny monoimidazole complex peaks at 52.5 and 16 ppm, the 7,13-CH_3 resonance of the bisimidazole complex at −9.5 ppm gives chemical exchange cross-peaks to the monoimidazole complex shoulder at 24 ppm, and the 2,18-CH_2 resonance of the bisimidazole complex at −10.7 ppm gives chemical exchange cross-peaks to the tiny monoimidazole complex peaks at 44.5 and 27 ppm. (b) EXSY spectrum of a mixture of [(Me_8C)FeCl] and its mono- and bisimidazole complexes recorded at 218 K in CD_2Cl_2. The 3,17-CH_3 resonance of the bisimidazole complex at 38 ppm gives chemical exchange cross-peaks to the tiny monoimidazole complex peak under the bound imidazole resonance at 63.5 ppm, the 8,12-CH_3 resonance of the bisimidazole complex at 12 ppm gives chemical exchange cross-peaks to the tiny monoimidazole complex peak at 76.6 ppm, the 7,13-CH_3 resonance of the bisimidazole complex at −5 ppm gives chemical exchange cross-peaks to the tiny monoimidazole complex peak under the resonance at 21.5 ppm, and the 2,18-CH_3 resonance of the bisimidazole complex at −9 ppm gives chemical exchange cross-peaks to the tiny monoimidazole complex peaks at 68 ppm.

parison, Fe(III) centers have ΔE_Q of more than 3 mm/s and isomer shifts of 0.3−0.4 mm/s,[32,39−46] although in all reported cases involving porphyrin ligands, the iron(III) center is a spin-admixed $S = 3/2$, 5/2 center, which may affect both parameters. A series of iron(III) phthalocyanines with halide or carboxylate anion as axial ligand have $\delta = 0.28-0.29$ mm/s and $\Delta E_Q = 2.94-3.12$ mm/s,[47] and are considered to be largely $S = 3/2$ systems, while the octaethyltetraazaporphyrinatoiron(III) chloride complex has two sites in the solid state, with $\delta = 0.37$ and 0.19 mm/s and $\Delta E_Q = 3.07$ and 3.00 mm/s,[48] respectively. The two sites are believed to differ in solvation near the iron.[48] Two 5-coordinate Fe(III) complexes with non-porphyrin N_4-donor macrocycles having pure $S = 3/2$ spin states have isomer shifts of 0.14[49] and 0.18[50] mm/s and quadrupole splittings of 3.63[49] and 3.56[50] mm/s. Thus, the Mössbauer parameters of [(Et_8C)-FeCl] ($\Delta E_Q = 2.99$ mm/s, $\delta = 0.19$ mm/s[8]) lie in the overlap region of those for Fe(III) and Fe(IV) complexes, and are likely more characteristic of an Fe(III) complex, on the basis of the isomer shift reported. In contrast, [(Et_8C)Fe(C_6H_5)] has a $\Delta E_Q = 3.72$ mm/s and $\delta = -0.11$ mm/s[8,23] and may, on the basis of the isomer shift, be an Fe(IV) complex. (The phenyl anion is a strong-field ligand and may be able to stabilize Fe(IV).) The 1-electron-reduced complex [(Et_8C)FePy] has a $\Delta E_Q = 3.88$ mm/s and $\delta = -0.09$ mm/s and therefore appears to be of the same metal oxidation and spin states. It was assigned the electron configuration iron(IV) corrole π anion radical on the basis of the similarity of the Mössbauer parameters to those of the chloroiron and phenyliron complexes.[8] However, it seems highly unlikely that a highly oxidized metal (Fe(IV)) would be stabilized in the presence of a highly reduced macrocycle (corrole π anion radical), as concluded by Vogel and coworkers,[8] and the NMR data of Table 2 are thus consistent with either a simple $S = 3/2$ Fe(III) formulation or a $S = 2$ iron(II) corrolate π cation radical in which the single macrocycle electron is antiferromagnetically coupled to the metal electrons. However, since this should lead to negative spin density, and downfield shifts of the *meso*-H resonances, as in the case of the manganese and chloroiron corrolates discussed above, and the iron(III) oxophlorins of ref 31, the upfield *meso*-H shifts (−95.1 and −82.8 ppm for $[(Me_8C)FeL_2]^+$ and −188.5 and −161.3 ppm for $[(Me_2Et_6C)FeL_2]^+$) rule out this possibility. Thus, the 1-electron-reduced chloroiron corrolates of this and the previous[8] study (Table 2) are clearly $S = 3/2$ Fe(III) complexes.

(43) Reed, C. A.; Mashiko, T.; Bentley, S. P.; Kastner, M. E.; Scheidt, W. R.; Spartalian, K.; Lang, G. *J. Am. Chem. Soc*. **1979**, *101*, 2948.
(44) Gupta, G. P.; Lang, G.; Reed, C. A.; Shelly, K.; Scheidt, W. R. *J. Chem. Phys*. **1987**, *86*, 5288.
(45) Gupta, G. P.; Lang, G.; Lee, Y. J.; Scheidt, W. R.; Shelly, K.; Reed, C. A. *Inorg. Chem*. **1987**, *26*, 3022.
(46) Reed, C. A.; Guiset, F. *J. Am. Chem. Soc*. **1996**, *118*, 3281.
(47) Kennedy, B. J.; Murray, K. S.; Zwack, P. R.; Homborg, H.; Kalz, W. *Inorg. Chem*. **1986**, *25*, 2539.
(48) Fitzgerald, J. P.; Haggerty, B. S.; Rheingold, A. L.; May, L.; Brewer, G. A. *Inorg. Chem*. **1992**, *31*, 2006.
(49) Kostka, K. L.; Fox, B. G.; Hendrich, M. P.; Collins, T. J.; Rickard, C. E. F.; Wright, L. J.; Mhnck, E. *J. Am. Chem. Soc*. **1993**, *115*, 6746.
(50) Keutel, H.; Käpplinger, I.; Jäger, E.-G.; Grodzicki, M.; Schhnemann, V.; Trautwein, A. X. *Inorg. Chem*. **1999**, *38*, 2320.

Table 5. Mössbauer Parameters of Some Fe(III) and Fe(IV) Complexes

compound	T (K)	OS[a]	S[b]	δ (mm/s)	ΔE_Q (mm/s)	ref
$[(TMP)Fe{=}O]^+Cl^-$	77	IV	1	0.06	1.62	35
[(TMP)Fe=O]		IV	1	0.04	2.3	36
[(OEP)Fe=O(Py)]	77	IV	1	0.10	+1.56	34
[(OEP)Fe=O(NMeIm)]	77	IV	1	0.11	+1.26	34
$[(TMP)Fe(OCH_3)_2]$	77	IV	1	−0.025	2.10	35
[(tetraamido-N)Fe(*t*-BuNC)$_2$][c]	4.2	IV	1	−0.04	3.38	38
$[(Et_8C)FeCl]$	77	III[d]	3/2, −1/2[d]	0.19	2.99	8
$[(Et_8C)Fe(C_6H_5)]$	77	IV?[e]	1?[e]	−0.11	3.72	8
$[(Et_8C)FePy]$	77	III[d]	3/2[d]	−0.09	3.88	8
$[(Et_8C)FeCl]ClO_4$	77	IV?[e]	1, −1/2?[e]	−0.10	3.66	23
$[(OEP)Fe(ClO_4)_2]$	4.2	III	3/2,5/2, −1/2	0.43	3.00	32
$[(TPP)Fe(ClO_4)]$	4.2	III	3/2, 5/2	0.38	3.43	43
$[(TP_{piv}P)Fe(OSO_2CF_3)(H_2O)]$	4.2	III	3/2, 5/2	0.43	2.2	42
$[(OEP)Fe(3\text{-}ClPy)]ClO_4$	4.2	III	3/2, 5/2	0.36	3.23	41
$[(TPP)Fe(B_{11}CH_{12})]\cdot C_7H_8$	4.2	III	3/2, 5/2	0.33	4.12	45
$[(OEP)Fe(EtOH)_2]ClO_4$	295	III	3/2, 5/2	0.29	2.97	41
	115			0.36	3.32	
	4.2			0.38	3.47	
$[(OEP)Fe(THF)_2]ClO_4$	298	III	3/2, 5/2	0.31	3.04	40
	77			0.42	3.34	
$[(TPP)Fe(FSbF_5)]$	4.2	III	3/2, 5/2	0.39	4.29	44
[(Pc)FeCl][f]	4.2	III	3/2, 5/2	0.28	2.94	47
[(Pc)FeI][f]	4.2	III	3/2, 5/2	0.28	3.23	47
[(OETAP)FeCl][g]	80	III	3/2	0.37[h] (73.8%)	3.07[h]	48
				0.19[h] (26.2%)	3.00[h]	
[(tetraamido-N)FeCl][c]	298	III	3/2	0.14	3.68	49
$[(N_4CTDT)FeI]$[I]	120	III	3/2	0.18	3.56	50

[a] Oxidation state of iron center. [b] Spin of iron center. [c] Tetraamido-N = 1,4,8,11-tetraaza-13,13-diethyl-2,2,5,5,7,7,10,10-octamethyl-3,6,9,12,14-pentaoxocyclotetradecanate(4−). [d] Oxidation and spin states listed as found by NMR spectroscopy in this work. Reference 8 reports oxidation state IV and $S = 1$. [e] Oxidation and spin state listed as reported in ref 8, but with some uncertainty based upon the present work (see the text). [f] Pc = phthalocyanine. [g] OETAP = octaethyltetraazaporphyrin. [h] Two Mössbauer signals observed; the two species are believed to differ in solvation near the iron. [i] N_4CTDT = 6,13-bis(ethoxycarbonyl)-5,14-dimethyl-1,4,8,11-tetraazacyclotetradeca-4,6,12,14-tetranate(2−).

An additional species, reported by the Vogel and Kadish groups, the 1-electron oxidized phenyliron corrole complex, $[(Et_8C)Fe(C_6H_5)]ClO_4$, has $\Delta E_Q = 3.66$ mm/s, $\delta = -0.10$ mm/s at 120 K, and an overall spin $S = 1/2$.[23] The similarity in quadrupole splittings of all of these iron corrolate species suggested to earlier workers[8,23] that they are all Fe(IV) centers. However, it now appears that the zero-field quadrupole doublet Mössbauer spectra of $S = 1$ Fe(IV) and $S = 3/2$ Fe(III) yield partially overlapping data, and it may well be that not all (and perhaps none) of the iron corrolate species for which Mössbauer spectra have been reported have Fe(IV) centers. On the basis of the NMR data presented herein, it is clear that the chloroiron complexes are iron(III) corrolate π cation radicals. And on the basis of the ambient temperature NMR data quoted in ref 8 for the iron phenyl complex of octaethylcorrole, the large range of the eight $-CH_2$ resonances (+98.1 to −8.4 ppm) and the fairly large positive *meso*-H shifts (54.5(2) and 49.3(1) ppm)[8] also suggest the electron configuration iron(III) corrolate π cation radical. The phenyl resonances (−4 ppm, *meta*; −77 ppm, *para*; −153.6 ppm, *ortho*) are intermediate between those of $[(TPP)Fe^{III}(C_6H_5)]$ (20 ppm, *meta*; −30 ppm, *para*; −100 ppm, *ortho*, measured at −60 °C) (a low-spin d^5 complex)[34] and $[(TPP)Fe^{IV}(C_6H_5)]^+$ (−80 ppm, *meta*; −142 ppm, *para*; −298 ppm, *ortho*, measured at −60 °C) (a $S = 1$ d^4 complex),[51] so it is possible that the iron phenyl corrolate is a resonance hybrid of these two iron oxidation and spin states. The low-temperature Mössbauer spectra, obtained in high applied magnetic fields, for all of the previously reported species[8,23] should be investigated, to clarify the spin and oxidation states of the iron in each complex and to set new guidelines for the ranges of quadrupole splittings and isomer shifts to be expected for $S = 3/2$ Fe(III) cation radicals of macrocycles as compared to $S = 1$ Fe(IV) macrocyclic complexes.

The room-temperature chemical shifts of the methyl and methylene protons of the 1-electron-reduced $S = 3/2$ iron(III) corrolates in pyridine solution (Table 2) provide a good measure of the range of shifts expected for a pure $S = 3/2$ iron(III) tetrapyrrole macrocycle complex in the absence of a macrocycle radical spin. The average *meso*-H shift is similar to that of $S = 5/2$ [(DPDME)FeCl], while the average pyrrole CH_3 shift is about 20 ppm larger than for the same complex.[28] (DPDME = deuteroporphyrin dimethyl ester.) And although iron corrolates having pyrrole H substituents have not been investigated, it is clear from the manganese corrolates that the very negative chemical shifts of the 2,18- and 3,17-H corrole protons (Table 2) indicate large π spin delocalization to the β-pyrrole positions 2,18 and 3,17. The chemical shifts of the pyrrole substituents of these 1-electron-reduced iron(III) corrolates also provide a good indication of the magnitude of the contribution of the macrocycle unpaired electron to the chemical shifts of the $S = 3/2$ chloroiron(III) corrolate cation radicals of Table 1. By subtracting the shifts of the iron(III) corrolates from those of the chloroiron corrolates, we find that the $7b_1$ orbital unpaired electron contributes 245 ppm to the *meso*-10-H, 188 ppm to the *meso*-5,15-H, −87.9 ppm to the pyrrole 2,18-CH_3, −38.2 ppm to the pyrrole 3,17-CH_3, +3.9 ppm to the pyrrole 7,13-CH_3, and −41.2 ppm to the pyrrole 8,12-CH_3. The magnitudes of the contributions to the chemical shifts of the manganese corrolate pyrrole and *meso* positions are approximately 25% of these, in the same order.

Electronic Structure of $[(Me_8C)Fe(imidazole)_2]Cl$ and $[(7,13\text{-}Me_2Et_6C)Fe(imidazole)_2]Cl$. EPR data (Figure 9) show a low-spin Fe(III) center for the bisimidazole complexes at low temperature. Binding of imidazole ligands does not appear to

(51) Balch, A. L.; Renner, M. W. *J. Am. Chem. Soc.* **1986**, *108*, 2603.

change the oxidation state of the iron center, but does change its spin state. It is unlikely that the Fe(III) π cation radical complexes are reduced to Fe(III) complexes upon the addition of axial ligands (i.e., there is no apparent redox reaction in the solution), since (a) the binding of imidazole ligands is reversible with temperature, (b) excess free ligand in the solution exhibits no change in its NMR spectrum with temperature, and (c) there is no other possible reductant in the solution. There is still an unpaired electron in the corrole ring, as evidenced by the large negative shifts of the *meso*-H resonances (Figures 5 and 8), although it is not detected in the EPR spectrum (Figure 9). A possible mechanism for the absence of evidence of the corrolate radical in the EPR spectrum is that the complexes form dimers in frozen solution at 4.2 K, as does vanadyl octaethylporphyrin cation radical,[52,53] and those of a number of other metal octaethylporphyrinate π cation radicals including that of $[(OEP)Zn(OH_2)]_2^{2+}$,[54,55] with the unpaired electrons in the two corrole rings antiferromagnetically coupled, resulting in a net spin of 1/2 (from low-spin Fe(III)) for each monomer. However, the metal−macrocycle spin coupling pattern is quite different for the vanadyl octaethylporphyrinate cation radical (strongly ferromagnetic)[52] and the low-spin iron(III) corrolate π cation radicals of the present study (probably weakly antiferromagnetic). Furthermore, it would not be possible to have complete overlap of the macrocycle rings in the present case, as observed for the $[(OEP)Zn(OH_2]_2^{2+}$ case,[54,55] because of steric interference from the axial imidazole ligands that are bound to the iron(III). Interestingly, the 6-coordinate $[(OEP)VO(OH_2)]_2^{2+}$ complex shows little if any overlap of the porphyrinate radical rings, yet strong antiferromagnetic coupling of the radical spins.[52]

However, in the temperature range of the NMR experiments (from −40 to −90 °C), there is no evidence of formation of dimers. When [(7,13-Me_2Et_6C)FeCl] and [(Me_8C)FeCl] are mixed and dissolved together and excess imidazole is added, no extra resonances are observed over the temperature range of the NMR measurements, suggesting that no additional species (i.e., a mixed-corrolate dimer) are formed unless they remain in rapid chemical exchange over the entire temperature range investigated. Thus, the iron corrolates bound to two imidazole ligands appear to be monomeric over the temperature range of the NMR measurements.

The chemical shifts of the alkylcorrolatoiron chloride complexes bound to two imidazole ligands, obtained in CD_2Cl_2 at −70 °C, are summarized in Table 3. The concentration of $[(Me_2Et_6C)Fe(ImH)_2]^+$ used to obtain these data was about 4 mM. The concentration of the $[(Me_8C)Fe(ImH)_2]^+$ sample was not measured, but was significantly lower than 1 mM because of the low and decreasing solubility of this complex with decreasing temperature; the imidazole concentration was about 15 mM in both samples. Although the chemical shifts of the complexes depend on the concentration of both the iron corrolate and imidazole (Figure 8), the upfield shifts of two of the pyrrole substituent protons are likely due in part to the effect of the dipolar shift, as expected from the rhombic EPR spectrum (Figure 9), if the largest g value is g_z, and indicate extremely small contact shifts at two ring positions, the 7,13-CH_3 position and the 2,18-CH_3 or -CH_2 position. Further analysis of the shifts is not possible because of their concentration dependence.

In contrast to the case of [(7,13-Me_2Et_6C)FeCl] and [(Me_8C)FeCl], $[(Me_8C)Fe(L)_2]^+Cl^-$ and $[(7,13\text{-}Me_2Et_6C)Fe(L)_2]^+Cl^-$ show large *upfield* shifts for the *meso*-H resonances, as mentioned above. As we have indicated, these large shifts cannot arise from σ spin delocalization. Instead, they must come from large positive π spin delocalization. Although Hückel calculations[16] show that there is a significant amount of π spin delocalization from the d_π orbitals of the iron center to the *meso* positions of the corrole (as compared to the corresponding porphyrin, which has practically zero spin delocalization to the *meso* positions), this spin density is not large enough to cause an upfield shift of −95 and −82.5 ppm (octamethylcorrolate) or −188 and −161 ppm (dimethylhexaethylcorrolate). Thus, the other contribution to this large spin density must be from the corrole ring unpaired electron. In this case there appears to be little coupling between the low-spin Fe(III) center electron and the π cation radical electron. Theory predicts a magnetic moment of[30]

$$\mu = [g_A{}^2 S_A(S_A + 1) + g_B{}^2 S_B(S_B + 1)]^{1/2} \quad \mu_B \qquad (2)$$

for a system having two uncoupled magnetic centers, A and B, where $g_A{}^2 = (1/3)(g_z{}^2 + g_y{}^2 + g_x{}^2)$ can be calculated from the g values of the iron center (Figure 9), and $g_B{}^2 \approx 4$ for the corrolate radical. The calculated magnetic moment is thus 2.59 μ_B, which should be unchanged over the temperature range of the NMR studies, once imidazole binding is complete (−50 to −90 °C). The magnetic susceptibility measurements discussed in the Results gave rise to a magnetic moment of 2.0 μ_B at −50 °C that decreased with decreasing temperature, probably due to low solubility and partial precipitation of the bisimidazole complex at low temperatures. The magnetic moment of 2.0 μ_B at −50 °C suggests that approximately 20−25% of the complex had precipitated at that temperature. The NMR shifts of the bisimidazole complexes are thus consistent with one unpaired electron each on the metal and the macrocycle, with uncoupled, or weakly coupled, spins. The difference in the *meso*-H shifts of $[(Me_8C)Fe(ImH)_2]^+$ and $[(Me_2Et_6C)Fe(ImH)_2]^+$ (Table 3) suggests weak antiferromagnetic (and different for the two complexes) coupling of the corrole spin to that of the metal, at least in the former case, where the shift is less negative, because large shifts of about −155 ppm at −50 °C are more consistent with a π cation radical, at least for porphyrins such as $[(OEP)Mg]^+$ (calculated from the EPR hyperfine coupling constant[56] and scaled to the temperature of the NMR measurement), and $[(OEP)Co]Br_2$ has a *meso*-H chemical shift of −100 ppm at 275 K, which would be about −132 ppm at −50 °C.[57] Although the spin densities at the *meso* positions of the corrole π cation radicals are undoubtedly somewhat different from those of the octaethylporphyrin π cation radicals, the difference in *meso*-H chemical shifts of the two bisimidazole iron corrolate complexes suggests some difference in the degree of magnetic coupling between the metal and macrocycle unpaired electrons for the two complexes.

The rhombic EPR spectrum of $[(Me_8C)Fe(ImH)_2]Cl$ shown in Figure 9 is typical of those for low-spin Fe(III) heme centers having $(d_{xy})^2(d_{xz},d_{yz})^3$ electron configurations, and the g values are typical for the above-mentioned ground state.[15,16] For this

(52) Schulz, C. E.; Song, H.; Lee, Y. J.; Mondal, J. U.; Mohanrao, K.; Reed, C. A.; Walker, F. A.; Scheidt, W. R. *J. Am. Chem. Soc.* **1994**, *116*, 7196.
(53) Lemtur, A.; Chakravorty, K.; Dhar, T. K.; Subramanian, J. *J. Phys. Chem.* **1984**, *88*, 5603.
(54) Song, H.; Reed, C. A.; Scheidt, W. R. *J. Am. Chem. Soc.* **1989**, *111*, 6865.
(55) Song, H.; Orosz, R. D.; Reed, C. A.; Scheidt, W. R. *Inorg. Chem.* **1990**, *29*, 4274.
(56) Fajer, J.; Borg, D. C.; Forman, A.; Dolphin, D.; Felton, R. H. *J. Am. Chem. Soc.* **1970**, *92*, 3451.
(57) Morishima, I.; Shiro, Y.; Takamuki, Y. *J. Am. Chem. Soc.* **1983**, *105*, 6168.

ground state, g_z is expected to be the largest g value, and the dipolar contribution to the isotropic shift of all corrolate resonances is thus expected to be negative,[16] as mentioned above with respect to the negative shifts of the 3,17 and 7,13 substituent resonances. The rhombicity of the EPR signal arises either from the axial imidazole ligands being in parallel or near-parallel planes or from the asymmetry of the corrolate ring, or both. In fact, the d_{xz} and d_{yz} orbitals cannot be degenerate because corrolates do not have C_{4v} or D_{4h} symmetry. From the g values, using the theory of Griffith[58] and the equations of Taylor,[59] the difference in energy of the d_{xz} and d_{yz} orbitals, the rhombic splitting, is calculated to be 3.29λ, where λ is the spin−orbit coupling constant.[60] As a result, we might expect anti-Curie behavior for the bisimidazole complexes due to a low-lying excited state. However, the difference of energy calculated from the NMR shifts using the two-level temperature dependence fitting program[61] (results not shown) does not match the EPR results, indicating that this system has several different processes going on simultaneously in solution, including this nondegeneracy of d_{xz} and d_{yz}, probably a weak antiferromagnetic coupling of metal and macrocycle unpaired electrons, and loss of imidazole ligands to produce the $S = 3/2$ Fe(III) π cation radical starting materials at higher temperatures, all of which contribute to the observed non-Curie behavior. Additional investigations of this complex utilizing low-temperature magnetic Mössbauer spectroscopy and magnetic susceptibility measurements are planned to more fully characterize the nature of the spin coupling between the low-spin Fe(III) and corrolate π cation radical electrons.

Acknowledgment. The support of the U. S. National Institutes of Health, Grant DK 31038 (F.A.W.), the Materials Characterization Program at the University of Arizona (F.A.W.), NATO, Grant CRG971495 (S.L.), and MURST (S.L.) is gratefully acknowledged. Thanks are due to Ms. Cadia D'Ottavi for her valuable technical assistance in the synthesis of the complexes, and to Dr. Arnold M. Raitsimring for EPR measurements.

Supporting Information Available: 1D and NOESY spectra of [(7,13-Me_2Et_6C)FeCl]. This material is available free of charge via the Internet at http://pubs.acs.org.

IC990784L

(58) Griffith, J. S. *Mol. Phys.* **1971**, *21*, 135.
(59) Taylor, C. P. S. *Biochim. Biophys. Acta* **1977**, *491*, 137.
(60) The calculated tetragonal splitting, $\Delta/\lambda = 5.35$, together with the rhombic splitting, $V/\lambda = 3.29$, yields a rhombicity (V/Δ) of 0.615, typical of the $(d_{xy})^2(d_{xz},d_{yz})^3$ electron configuration.[15,16,59]
(61) Shokhirev, N. V.; Walker, F. A. *J. Phys. Chem.* **1995**, *99*, 17795.